Natural Computing (2021) 20:329–340
https://doi.org/10.1007/s11047-021-09842-6

Counting infinitely by oritatami co-transcriptional folding

Kohei Maruyama[1] · Shinnosuke Seki[1,2]

Accepted: 8 January 2021 / Published online: 11 March 2021

Abstract
A fixed bit-width counter was proposed as a proof-of-concept demonstration of the oritatami model of cotranscriptional folding [Geary et al., Proc. MFCS 2016, LIPIcs 58, 43:1-43:14], and it was embedded into another oritatami system that self-assembles a finite portion of Heighway dragon fractal. In order to expand its applications, we endow this counter with capability to widen bit-width at every encounter with overflow.

Keywords Theory of algorithmic molecular self-assembly · RNA cotranscriptional folding · Oritatami system · Counting

1 Introduction

Counting is one of the most essential tasks for computing. Nature has been counting billions of days using molecular "circadian clockwork" which is "as complicated and as beautiful as the wonderful chronometers developed in the 18th century" (McClung 2006). Nowadays, developments in molecular self-assembly technology enable us to design molecules to count. Evans has demonstrated a DNA tile self-assembly system that counts accurately *in-vitro* in binary from a programmed initial value until it overflows (Evans 2014). In its foundational theory of molecular self-assembly, such binary counters have been proved versatile, being used to assemble shapes of particular size (Adleman et al. 2001; Rothemund and Winfree 2000), towards self-assembly of fractals (Masuda et al. 2018), and as an infinite scaffold on which Turing machines can be simulated in parallel in the abstract tile-assembly model (Bryans et al. 2013; Lathrop et al. 2011), to name a few.

A fixed bit-width (finite) binary counter has been implemented as a proof-of-concept demonstration of the oritatami model of cotranscriptional folding (Geary et al. 2019). As shown in Fig. 1, an RNA transcript folds upon itself while being transcribed (synthesized) from its corresponding DNA template strand. Geary, Rothemund, and Andersen programmed a specific RNA rectangular tile structure into a DNA template in such a way that the corresponding RNA transcript *folds cotranscriptionally* into the programmed tile structure with high probability *in-vitro* at room temperatures (*RNA origami*) (Geary et al. 2014). An oritatami system folds a transcript of abstract molecules called *beads* of finitely many types over the 2-dimensional triangular lattice cotranscriptionally according to a rule set that specifies which types of molecules are allowed to bind at unit distance. The transcript of the binary counter in Geary et al. (2019) is of period 60 as ⓪ − ① −⋯− ㊾ − ⓪ −⋯ and its period is divided semantically into two half-adder (HA) modules A = ⓪ − ① − ⋯⋯ − ⑪ and C = ㉚ − ㉛ − ⋯⋯ − ㊶ and two structural modules B and D, which are sandwiched by half-adder modules along the transcript as $ABCD$. While being folded cotranscriptionally in zigzags, HA modules increment the current counter value i by 1, which is initialized on a linear *seed* structure, alike the Evans' counter, whereas structural modules B and D align HA modules properly and also make a turn at an end of the counter value i; B guides the transcript from a zig to a zag (↪) while D does from a zag to a zig (↩). This counter was

An extended abstract on this work was published as a short paper in the proceedings of the 46th International Conference on Current Trends in Theory and Practice of Computer Science (SOFSEM 2020, Limassol, Cyprus, January 20-24, 2020), Lecture Notes in Computer Science (LNCS) 12011, pp. 566–575.

✉ Shinnosuke Seki
s.seki@uec.ac.jp

[1] The University of Electro-Communications, 1-5-1 Chofugaoka, Chofu, Tokyo 1828585, Japan

[2] École Normale Supérieure de Lyon, 46 allée d'Italie, 69007 Lyon, France

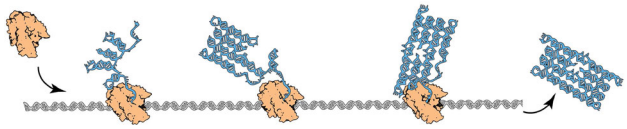

Fig. 1 RNA origami. RNA polymerase enzyme (orange) synthesizes the temporal copy (blue) of a gene (gray spiral) out of ribonucleotides of four types A, C, G, and U

embedded as a component of an oritatami system to self-assemble an arbitrary finite portion of Heighway dragon fractal (Masuda et al. 2018); it remembers how many turns the dragon has made so far. Its applications are limited, however, by lack of mechanism to detect an overflow, at which its behavior is undefined and it gets nondeterministic. In this paper, we shall endow this counter, or more precisely, its structural module B, with the capability of overflow detection and bit-width expansion thereof.

The oritatami model has been proven Turing universal in Geary et al. (2018), where a universal Turing machine is encoded as a seed and a period of transcript of an oritatami system using 542 bead types via cyclic tag system, and the number of bead types needed for the universality was reduced to almost one-third (183 bead types) recently (Pchelina et al. 2020) by an intrinsic simulation of 1-dimensional cellular automata (CA). It is hence no surprise that oritatami systems can count even infinitely. In the read-once-write-once models of computation such as oritatami, abstract tile-assembly model (aTAM) (Rothemund and Winfree 2000; Winfree 1998), and many others in molecular self-assembly, however, what a computation matters is not so much an output obtained conclusively but rather a shape self-assembled in the course; the shape is often the goal of computation in molecular self-assembly. Unless being interlocked geometrically, the output cannot wire to an input of another computation. The versatile systems in oritatami (Geary et al. 2018; Pchelina et al. 2020) hence never discourage us to design a set of singly-functional modules of simple enough shape to be wired, preferably via a common interface. (Note that unless being provided anyhow with random access memory, in molecular self-assembly, the ability to count highly unlikely suffices for Turing universality; c.f. Minsky 1967.)

The proposed counter is simple in number of bead types used as well as length of its transcript period. It transcribes ①−②−⋯−㉜ repetitively (needless to say, 132 bead types), whereas the period of a transcript to simulate a radius-r CA with Q states by the simplified Turing universal oritatami system (Pchelina et al. 2020) is of length about $\frac{142}{3} Q_r^2 \log_2 Q_r$, where $Q_r = 2^{\lceil \log_2 (2Q^{2r+1}) \rceil}$, whose value cannot be smaller than $\frac{142}{3} \cdot 4 \geq 189$, obtained at $Q = 1$ and $r = 0$, and rises significantly in order for CAs to be able to compute as $\frac{142}{3} \cdot 4 \cdot 16^2 \geq 48469$ at $Q = 2$ and $r = 1$. A periodic transcript is expected to be transcribed from a circular DNA (Geary and Andersen 2014) but such a template DNA sequence gets more costly to be synthesized as it gets longer. The proposed counter folds in zigzags into a logarithmically-widening trapezoid so that it cannot be afforded at any scaling of Heighway dragon fractal. It therefore does not truly enable to self-assemble this fractal. The significance of this counter is rather to demonstrate that an oritatami system can detect an overflow and change its phase therein from counting to bit-expansion and back (note that oritatami is not provided with any internal states; see Sect. 2). This phase-transition capability should be applicable, for example, to self-assemble the $n \times n$ square in oritatami at a scale, starting from an $O(\log n)$-size seed encoding n, based on the system in aTAM for square self-assembly (Rothemund and Winfree 2000); such a system would make use of this capability rather to transition from the binary counting phase to the phase to fill the remaining $n \times (n - \log n)$ rectangle while drawing the diagonal.

This paper is organized as follows. In Sect. 2, we provide basic notions and notation of oritatami system. The infinite counter shall be explained into detail in Sect. 3. We conclude this paper in Sect. 4 with a short discussion.

2 Preliminaries

Let Σ be a finite alphabet, whose elements should be regarded as types of abstract molecule, or *beads*. A bead of type $a \in \Sigma$ is called an a-bead. By Σ^* and Σ^ω, we denote the set of finite sequences of beads and that of one-way infinite sequences of beads, respectively. The empty sequence is denoted by λ. Let $w = b_1 b_2 \cdots b_n \in \Sigma^*$ be a sequence of length n for some integer n and bead types $b_1, \ldots, b_n \in \Sigma$. The *length* of w is denoted by $|w|$, that is, $|w| = n$. For two indices i, j with $1 \leq i \leq j \leq n$, we let $w[i..j]$ refer to the subsequence $b_i b_{i+1} \cdots b_{j-1} b_j$; if $i = j$, then $w[i..i]$ is simplified as $w[i]$. For $k \geq 1$, $w[1..k]$ is called a *prefix* of w.

Oritatami systems fold their transcript, which is a sequence of beads, over the triangular grid graph $\mathbb{T} = (V, E)$ cotranscriptionally. A directed path $P = p_1 p_2 \cdots p_n$ in $\mathbb{T}$ is a sequence of *pairwise-distinct* points $p_1, p_2, \ldots, p_n \in V$ such that $\{p_i, p_{i+1}\} \in E$ for all $1 \leq i < n$. Its i-th point is referred to as $P[i]$. Now we are ready to abstract RNA single-stranded structures in the name of conformation. A *conformation* C (over Σ) is a triple (P, w, H) of a directed path P in $\mathbb{T}$, $w \in \Sigma^*$ of the same length as P, and a set of (hydrogen) bonds $H \subseteq \big\{\{i,j\} \;\big|\; 1 \leq i, i+2 \leq j, \{P[i], P[j]\} \in E\big\}$. This is to be interpreted as the sequence w being folded along the path P in such a manner that its i-th bead $w[i]$ is placed at the i-th

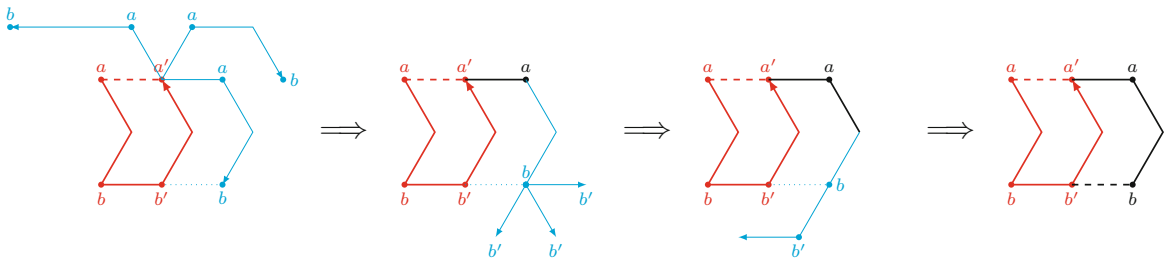

Fig. 2 Folding of a glider motif by a delay-3 deterministic oritatami system

point $P[i]$ and the i-th and j-th beads are bonded (by a hydrogen-bond-based interaction) if and only if $\{i,j\} \in H$. The condition $i+2 \leq j$ represents the topological restriction that two consecutive beads along the path cannot be bonded. A *rule set* $R \subseteq \Sigma \times \Sigma$ is a symmetric relation over Σ, that is, for all bead types $a, b \in \Sigma$, $(a,b) \in R$ implies $(b,a) \in R$. A bond $\{i,j\} \in H$ is *valid with respect to* R, or simply R-valid, if $(w[i], w[j]) \in R$. This conformation C is *R-valid* if all of its bonds are R-valid. For an integer $\alpha \geq 1$, C is *of arity* α if it contains a bead that forms α bonds but none of its beads forms more. By $\mathcal{C}_{\leq \alpha}(\Sigma)$, we denote the set of all conformations over Σ whose arity is at most α; its argument Σ is omitted whenever Σ is clear from the context.

The oritatami system grows conformations by an operation called elongation. Given a rule set R and an R-valid conformation $C_1 = (P, w, H)$, we say that another conformation C_2 is an elongation of C_1 by a bead $b \in \Sigma$, written as $C_1 \xrightarrow{R} bC_2$, if $C_2 = (Pp, wb, H \cup H')$ for some point $p \in V$ not along the path P and set $H' \subseteq \{\{i, |w|+1\} \mid 1 \leq i < |w|, \{P[i], p\} \in E, (w[i], b) \in R\}$ of bonds formed by the b-bead; this set H' can be empty. Note that C_2 is also R-valid. This operation is recursively extended to the elongation by a finite sequence of beads as: for any conformation C, $C \xrightarrow{R} \lambda^* C$; and for a finite sequence of beads $w \in \Sigma^*$ and a bead $b \in \Sigma$, a conformation C_1 is elongated to a conformation C_2 by wb, written as $C_1 \xrightarrow{R} wb^* C_2$, if there is a conformation C' that satisfies $C_1 \xrightarrow{R} w^* C'$ and $C' \xrightarrow{R} bC_2$.

An *oritatami system* Ξ is a tuple $(\Sigma, R, \delta, \alpha, \sigma, w)$, where Σ and R are defined as above, while the other elements are a positive integer δ called *delay*, a positive integer α called *arity*, an initial R-valid conformation $\sigma \in C_{\leq \alpha}(\Sigma)$ called the *seed*, and a (possibly infinite) *transcript* $w \in \Sigma^* \cup \Sigma^\omega$, which is to be folded upon the seed by stabilizing beads of w one at a time so as to minimize energy collaboratively with the succeeding $\delta - 1$ nascent beads. The energy of a conformation $C = (P, w, H)$, denoted by $\Delta G(C)$, is defined to be $-|H|$; the more bonds a conformation has, the more stable it gets. The set $\mathcal{F}(\Xi)$ of conformations *foldable* by the system Ξ is recursively defined as: the seed σ is in $\mathcal{F}(\Xi)$; and provided that an elongation C_i of σ by the prefix $w[1..i]$ be foldable (i.e., $C_0 = \sigma$), its further elongation C_{i+1} by the next bead $w[i+1]$ is foldable if

$$C_{i+1} \in \arg\min_{\substack{C \in \mathcal{C}_{\leq \alpha} s.t. \\ C_i \xrightarrow{R} w[i+1]C}} \min\left\{ \Delta G(C') \;\middle|\; \begin{array}{c} C \xrightarrow{R} *_{w[i+2..i+k]} C', \\ k \leq \delta, C' \in \mathcal{C}_{\leq \alpha} \end{array} \right\}. \tag{1}$$

Then we say that the bead $w[i+1]$ and the bonds it forms are *stabilized* according to C_{i+1}. Note that an arity-α oritatami system cannot fold any conformation of arity larger than α. A conformation foldable by Ξ is *terminal* if none of its elongations is foldable by Ξ. The oritatami system Ξ is *deterministic* if for all $i \geq 0$, there exists at most one C_{i+1} that satisfies (1). A deterministic oritatami system folds into a unique terminal conformation.

Example 1 (Glider[1]) See Fig. 2 for a delay-3 deterministic oritatami system Ξ to fold a motif called a glider. Its transcript is a repetition of $a \bullet bb' \bullet a'$ and its rule set R is $\{(a,a'), (b,b')\}$. Its seed is colored in red. The first 3 beads, $a \bullet b$, are transcribed and elongate the seed in all possible ways. The a-bead cannot bind or the second bead is inert according to R. The third bead, b, can bind to the b'-bead in the seed but for that, the a-bead must be located to the east of the previous a'-bead; it is thus stabilized there. Then the next bead, b', is transcribed. After the three steps, the third bead, b, is stabilized, along with its bond with the b'-bead, yielding the rightmost glider of width 3 and height 3 in Fig. 2. In the next 3 steps, the succeeding $b' \bullet a'$ folds alike and results in a glider of width 4 and height 3. The glider thus proceeds by unit distance per three beads and one bond.

The glider is self-sustaining and has provided a solid scaffold to oritatami systems (Demaine et al. 2018; Elonen 2016; Geary et al. 2018; Han and Kim 2018; Pchelina et al.

[1] A video to show how a glider folds can be found at https://www.dailymotion.com/video/x3cdj35, in which the Turing universal oritatami system by Geary et al. (2018) is running at delay 3.

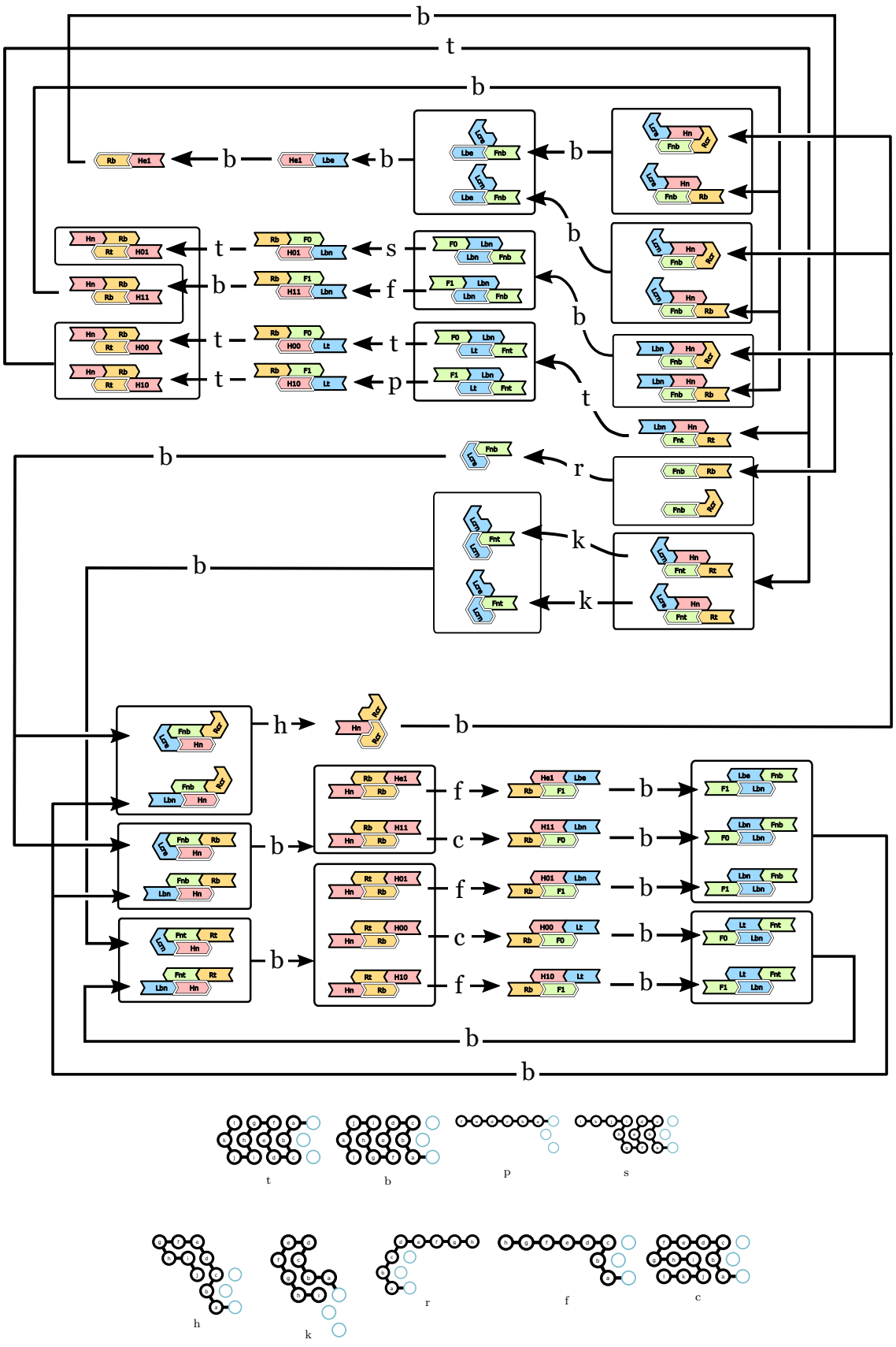
t
b
p
s
h
k
r
f
c

◀**Fig. 3** A brick automaton of the proposed infinite binary counter. 9 possible ways of folding the first several beads of a module being transcribed are enumerated at the bottom with labels t, b, ..., and transitions in the brick automaton are labeled with a corresponding way of folding

1– 30	Format module or F; colored in green
31– 66	Left-Turn module or L; blue
67– 96	Half-Adder module or H; red
97–132	Right-Turn module or R; yellow

2020). Counting infinitely in a zigzag manner requires a self-sustaining structure in order to travel "in a vacuum," that is, in the absence of the previous zag above, while widening bit-width at an overflow (see Figs. 11 and 12). Thanks to the sparsity of bonds, gliders can be deformed so easily for us to design multifunctional modules for the proposed counter. However, the bond density does not always determine the degree of functional extensibility; indeed, parallelograms, based on which the fixed bit-width counter (Geary et al. 2019) was designed, have turned out to be highly functionally extensible (Geary et al. 2018; Pchelina et al. 2020), in spite of relatively larger number of bonds necessary.

3 Folding an infinite binary counter

In this section, we describe a delay-3, arity-5 deterministic oritatami system to count infinitely. It employs 132 bead types, and its transcript w is a repetition of 1-2-3- ⋯ -132. Its rule set is given in Sect. 3.6. The fixed bit-width counter by Geary et al. (2019) operates at delay 4 under a different dynamics, but it was modified in Masuda et al. (2018) so as to run at delay 3 and under the more prevailing dynamics (1) in the research of oritatami model.

3.1 General idea

Between two consecutive overflows, the proposed system behaves in the same way as the fixed bit-width counter. Its transcript folds in a zigzag manner macroscopically (downward in figures throughout this paper). A zig, folding from right to left, increments the current counter value by 1. The succeeding zag, folding from left to right, formats the incremented counter value for the sake of next zig and copies it downward. Unlike the existing counter, when a zig encounters an overflow, it does not abort but rather extends the bit-width of the current counter value by 1 bit.

The transcript of the proposed counter is periodic. Its period 1-2-3- ⋯ -132 is divided semantically into the following four subsequences, called *modules*:

The transcript can be hence represented as $(\mathrm{FLHR})^*$ at the modular level. Modules are to play their roles in expected environments by folding into respective conformations which should be pairwise-distinct enough to be distinguishable by other modules transcribed later. Such expected conformations are called a *brick*. For example, module F encounters the four environments shown in Fig. 4 where it takes the four bricks Fnt, Fnb, F0, and F1, respectively. Here, by saying (an instance of) a module folds into (or takes) a brick in an environment, what we actually mean is that the rule set is designed so as for the transcript of the module to interact with itself as well as with the environment and fold deterministically into that brick according to the dynamics (1). The whole system is designed to guarantee that each module is transcribed only in one of the environments it expects. This fact is illustrated in the *brick automaton* in Fig. 3, which describes pairs of an environment and a brick as a vertex and transitions between them, introduced in Geary et al. (2019). Since this automaton is closed, it suffices to test whether for all pairs of an environment and a brick, the brick is folded deterministically in the environment. This test has been done *in-silico* using a simulator developed for this project. This brick automaton and all the certificates can be found at https://komaruyama.github.io/oritatami-infinit-counter/.

Seed and Encoding. An initial counter value is encoded in binary as $b_{k-1}b_{k-2}\cdots b_1b_0$ on the seed in the following format:

$$64\text{–}65\text{–}66\text{–}\left(\prod_{i=k-1}^{0}\left(w_{Hn}w_{Rb}w_{Fb_i}w_{Lbn}\right)\right)w_{Hn}, \tag{2}$$

where

$$\begin{aligned}
w_{Hn} &= 67\text{–}76\text{–}77\text{–}78\text{–}79\text{–}88\text{–}89\text{–}90\text{–}91\text{–}96,\\
w_{Rb} &= 97\text{–}102\text{–}103\text{–}108\text{–}109\text{–}114\text{–}115\text{–}120\text{–}\\
&\quad\ \text{–}121\text{–}126\text{–}127\text{–}132,\\
w_{F0} &= 1\text{–}10\text{–}11\text{–}12\text{–}13\text{–}22\text{–}23\text{–}24\text{–}25\text{–}30,\\
w_{F1} &= 1\text{–}22\text{–}23\text{–}24\text{–}25\text{–}26\text{–}27\text{–}28\text{–}29\text{–}30,\\
w_{Lbn} &= 31\text{–}36\text{–}37\text{–}42\text{–}43\text{–}48\text{–}49\text{–}54\text{–}55\text{–}64\text{–}\\
&\quad\ \text{–}65\text{–}66.
\end{aligned}$$

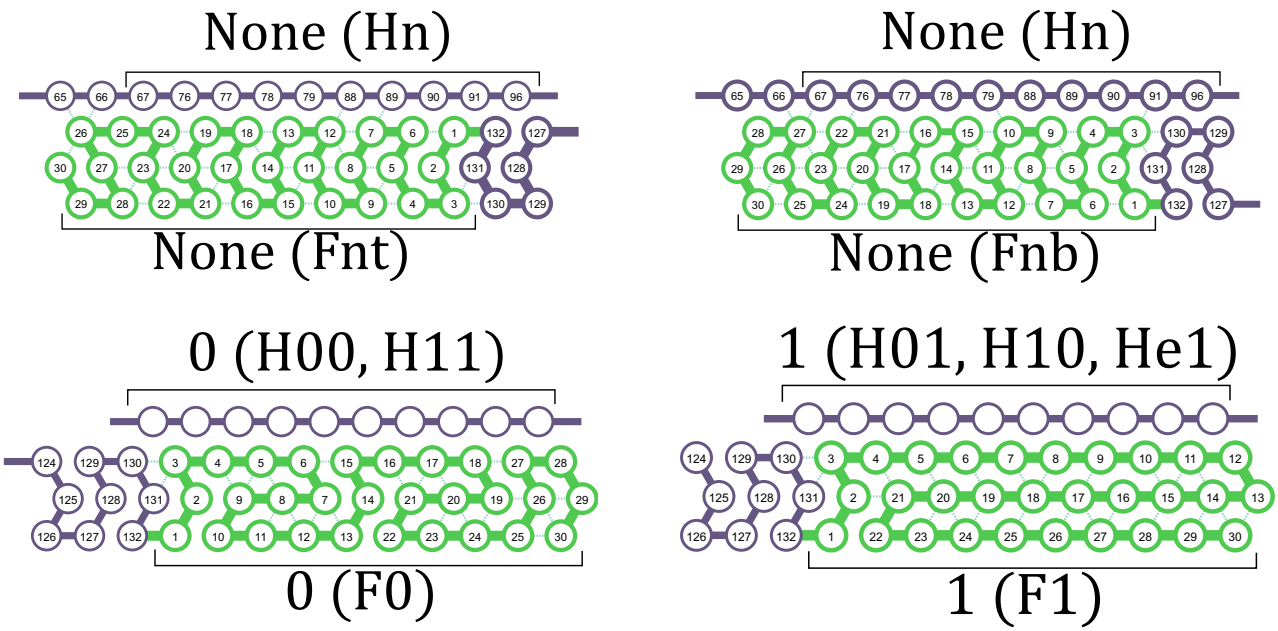

Fig. 4 All the four bricks of module F: The two bricks at the top, `Fnt` and `Fnb`, are for zigs while the others, `F0` and `F1`, are for zags. `Fnb` binds to the zag above so weakly that it can fold even in the absence of such a zag, that is, at an overflow

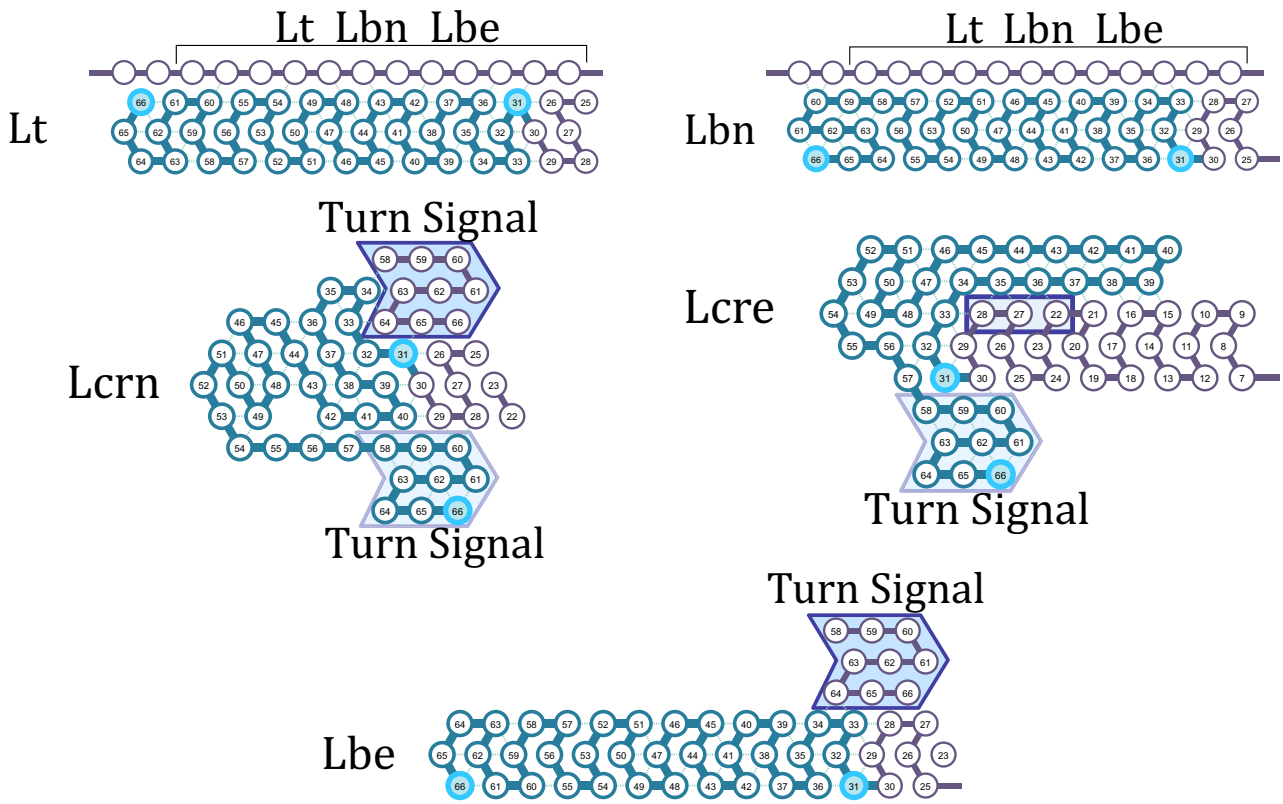

Fig. 5 All the five bricks of module L: `Lt`, `Lbn`, `Lcrn`, `Lcre`, and `Lbe` from top left to bottom right. In zigs, L folds into either `Lt` or `Lbn` depending on where it starts, until the transcript reaches the left end, where L folds either into `Lcrn` if the current counter value has not been overflowed, or into `Lbe` at an overflow. In the case of overflow, the next L folds into `Lcre`. In zags, L always folds into `Lbn`

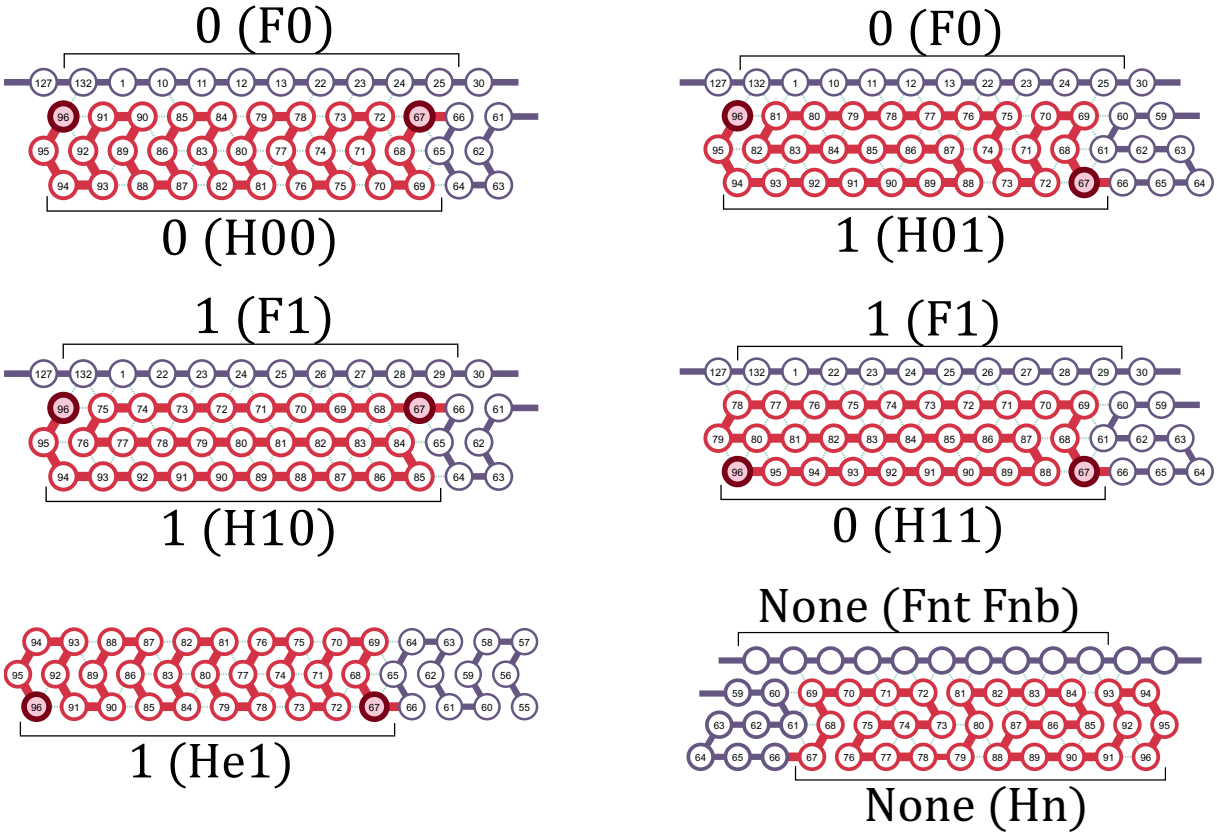

Fig. 6 All the six bricks of module H: `H00`, `H01`, `H10`, `H11`, `He1`, and `Hn` from top left to bottom right. In zags, H always folds into `Hn` while in zigs, it folds into one of the other five bricks

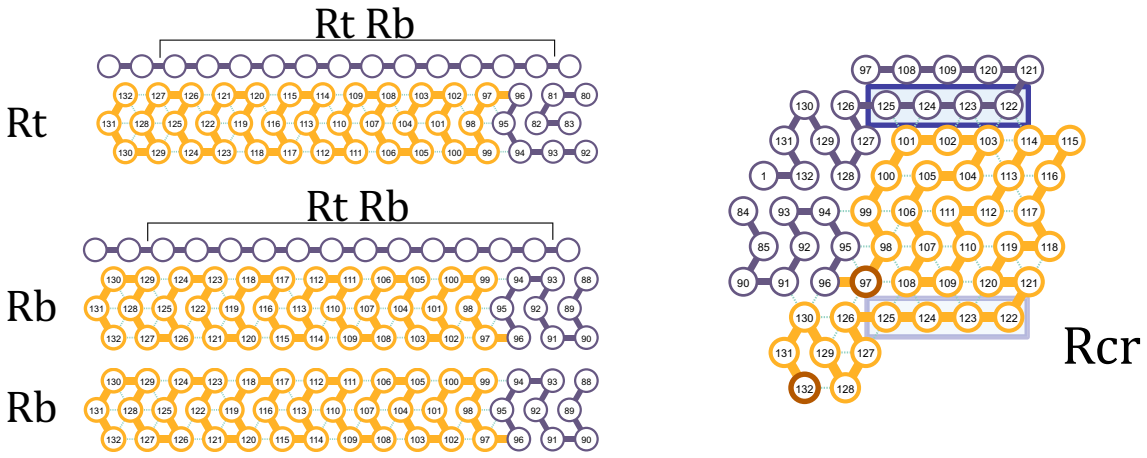

Fig. 7 All the three bricks of module R: `Rt`, `Rb`, and `Rcr`. In zigs, R folds into `Rt` or `Rb`, depending on how high it starts. In zags, R always folds into `Rb` until the transcript reaches the right end, where R folds into `Rcr` due to the four beads (boxed). `Rcr` is provided with this Turn Signal for the next right carriage-return. Note that `Rb` is not bonded to the environment at all. That is, this module certainly folds into `Rb` at an overflow

w_{Hn}, w_{Rb}, w_{F0}, w_{F1}, and w_{Lbn} are sequences of bead types exposed downward by modules H, R, F, L when they fold into bricks `Hn`, `Rb`, `F` b_i, `Lbn`, respectively, which can be found in Figs. 6, 7, 4, and 5 . The seed consists of the initial value encoded as (2), preceded by the sequence 58−59−60−61−62−63 folded into a glider-shaped signal for left turn, and succeeded by 97−108−109−120−122−123−· · ·131−132 that folds as the

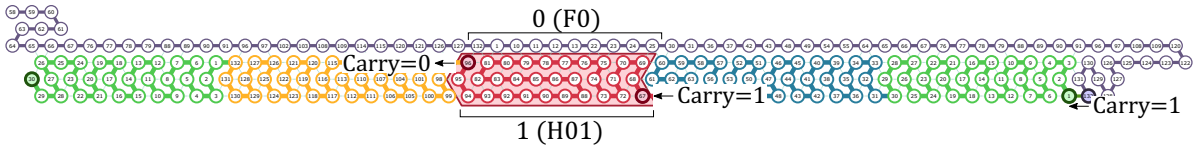

Fig. 8 The first zig. The initial counter value 0 is encoded below the seed in the format (2) with $k = 1$ (1-bit width). Being fed with carry, the zig increments the count. Module H outputs 1, or more precisely a sequence of bead types which shall be interpreted as 1 in the next zag and reformatted, as a sum and cancels the carry

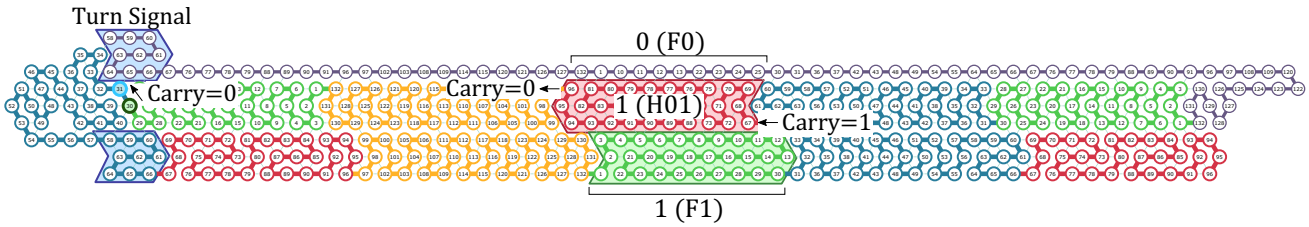

Fig. 9 The first zag. A Turn Signal at the left end of the seed makes module L folds into the brick Lcrn to turn and initiate the zag. This brick is equipped with another Turn Signal for the sake of the next turn. In a zag, module F reads the output of module H from above and formats it for the sake of the next zig

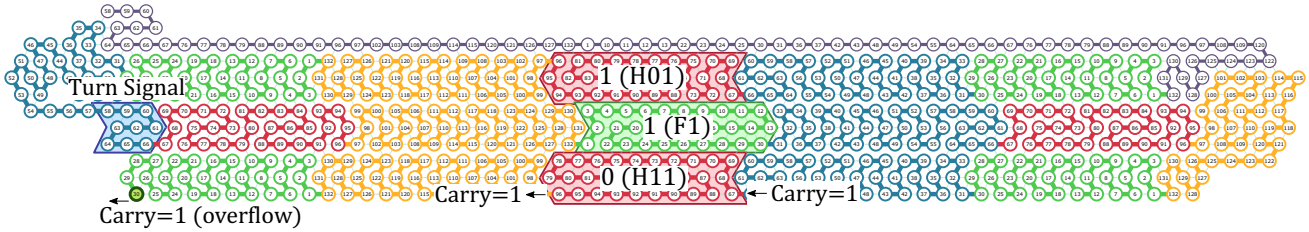

Fig. 10 Overflow. When the carry has not been canceled out until the end of a zig, the Turn Signal is too far for the upcoming module, which is L, to be folded into the brick Lcrn for turn

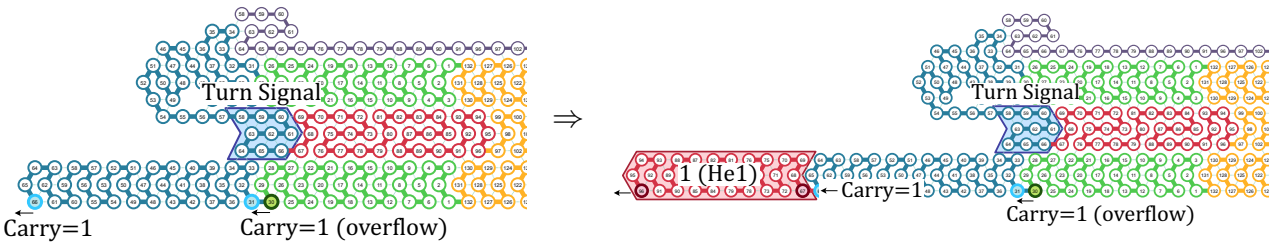

Fig. 11 (Left) Starting from the bottom, the Turn Signal above is too far for this L to fold into `Lcrn`. It rather folds into `Lbe` and initiates bit expansion. (Right) Without anything around, the succeeding H folds into a glider (brick `He1`)

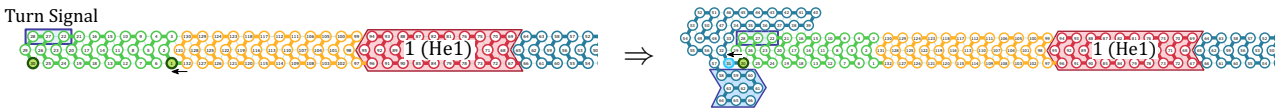

Fig. 12 The succeeding R and F also fold into respective glider-like bricks. (Left) This brick of F (`Fnb`) exposes Turn Signal `28-27-22` (boxed), which is usually "hidden" under the previous zag. (Right) The exposed `28-27-22` (boxed) triggers the folding of next L into a special brick (`Lcre`) for left carriage-return

module R folds into a brick `Rcr` (see Fig. 7). The seed is exemplified for $k = 1$ and $b_0 = 0$ in Fig. 8 or for $k = 0$ (non-coding, i.e., initial counter value 0) in Fig. 13, where it is colored in purple.

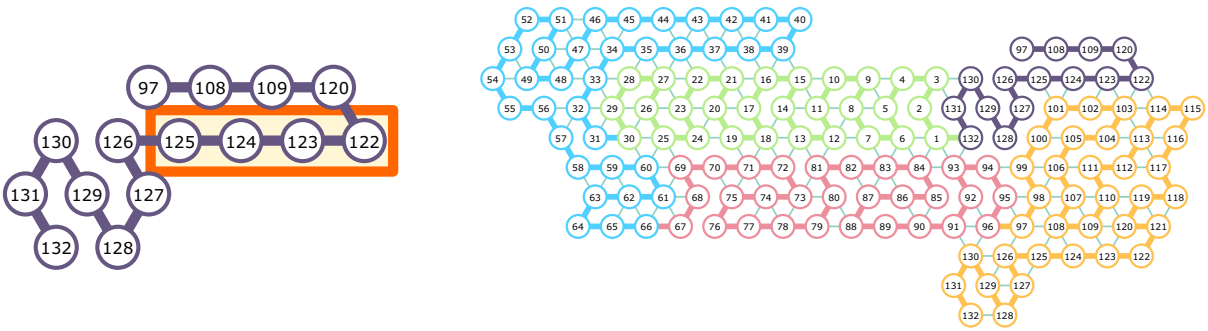

Fig. 13 Counting from a non-coding seed. (Left) The simplest-possible seed that consists only of the boxed right Turn Signal. (Right) Starting from this non-coding seed, the first period results in the counter value 1 in the 1-bit

3.2 Brick level overview

Starting from the seed, this system cyclically transits four phases: zig (←), left carriage-return (↪), zag (→), and right carriage-return (↩). The prefix $(\mathrm{FLHR})^k\mathrm{F}$ of the transcript folds into the first zig (recall that k is the bit-width of the initial count). In zigs in general, all the instances of modules F and H fold into bricks of width 10 and height 3, while those of L and R fold into bricks of width 12 and height 3. Zigs thus turn out to be a linear structure of height 3. We can inductively observe that the i-th instance of H in the prefix is transcribed right below b_{i-1} encoded on the seed in the format (2) so that the H can "read" b_{i-1}. After the whole prefix has thus folded into the first zig, the next L is transcribed right below Turn Signal, which lets the L fold into a special brick for left carriage-return if the zig ended at the top (this occurs unless $b_{k-1} = b_{k-2} = \cdots = b_0 = 1$) (see Fig. 9). We should note that this special brick `Lcre` is provided with another Turn Signal for the sake of next left carriage-return (see Fig. 5). Having been thus carriage-returned, the succeeding subsequence $(\mathrm{HRFL})^k\mathrm{H}$ of the transcript folds into the first zag. Even in zags, F and H fold into bricks of width 10 and height 3, while L and R fold into bricks of width 12 and height 3. As a result, zags turn out also to be a linear structure of height 3. More importantly, instances of H and F are aligned thus vertically and alternately into columns (see Figs. 8, 9, and 10), i-th of which from the right propagates the $(i-1)$-th bit of the counter value downward. After the whole subsequence has folded into the first zag, an instance of R is transcribed and folded into a special brick `Rcr` for right carriage-return due to the Turn Signal `125-124-123-122`, which occurs also at the bottom of `Rcr` (see Fig. 7) for the sake of next right carriage-return. This amounts to one cycle of the phase transition.

3.3 Increment of the counter

In a zig, module H plays its primary role as a half-adder and carry transfers through instances of others (F, L, and R) from an instance of H to another for more significant bit. Carry transfers as a height for modules to start. In zigs, modules F, L, and R take the respective two bricks (`Fnt` and `Fnb` for F, `Lt` and `Lbn` for L, and `Rt` and `Rb` for R; see Figs. 4, 5, and 7), both of which start and end at the same height: one at the top while the other at the bottom. A zig is fed with carry by being forced to start at the bottom by the last `Rcr` or the seed. Until an overflow, module H encounters only four environments, which encode input 0 as w_{F0} or 1 as w_{F1} and carry or no-carry as of whether the module starts at the bottom or top, where it takes `H00`, `H01`, `H10`, and `H11`, respectively, as shown in Fig. 6 (Hxc is folded when the input is x and the carry is given if $c = 1$ or not otherwise).

Let us see how the subsequence $(\mathrm{FLHR})^k\mathrm{F}$ folds into a zig in order to count up; for $k = 1$ and the current counter value 0, see Fig. 8. The zig starts at the bottom, that is, being carried, and the carry transfers through the first instances of F and L in the way just explained toward the first instance of H. This H is thus fed with carry and folds into `H01` if the bit encoded above is 0, as illustrated in Fig. 8, or `H11` if the bit is rather 1. `H01` ends at the top, corresponding to canceling the carry out. This absence of carry transfers through the succeeding modules leftward. As a result, the zig, or more precisely, the last instance of F of the subsequence ends folding at the bottom if this increment causes an overflow (Fig. 10), or at the top otherwise (Fig. 8). An instance of L is to be transcribed next. It folds either into `Lcrn` for carriage-return unless the counter value is overflowed, or into `Lbe` at an overflow.

3.4 Bit-width expansion at an overflow

The fixed bit-width counter (Geary et al. 2019) cannot handle a zig that ends at the bottom, that is, its behavior is

undefined, that is, it gets nondeterministic, at an overflow. In contrast, module L in this infinite counter is designed so as to fold into `Lbe` in this situation in order to keep counting up (Fig. 11). Observe that the dent on Turn Signal made of `58`, `63`, and `64` is too far for module L, or more precisely, for its beads `33` and `34` to interact with strongly enough to fold into `Lcrn`. `Lbe` is a self-sustaining conformation (glider) so that it can fold even in a "void," which occurs at that very moment. For the same reason, the following instances of H, R, and F fold into self-sustaining conformations `He1`, `Rb`, and `Fnb`, respectively (Figs. 11 and 12). Note that `He1` is essentially the same as `H00` but exposes the opposite side downward, which will be interpreted as the leading bit 1 after expansion in the next zag. When the next instance of L is transcribed, there is nothing around. Nevertheless, it does not fold into `Lbe` but folds into `Lcre` for carriage-return; how? It is guided by interaction between the beads `35`, `36` along the transcript of L and the Turn Signal `28-27-22` above `Fnb` (Figs. 5 and 12). This signal is usually hidden geometrically by the previous zag, and hence, does no harm.

3.5 Formatting

The counter value has been successfully incremented but the resulting value is not in the format (2) yet. A subsequence $(\mathrm{HRFL})^k\mathrm{H}$ of the transcript folds into the next zag, where k is the bit width of the incremented counter value. In this zag, instances of F play their primary role to format the 1-bit output by module H (recall that instances of H and F are aligned vertically and alternately) so as to expose the incremented counter value in the format (2) for the next zig. Both of the bricks of L for carriage-return, i.e., `Lcrn` and `Lcre`, end at the bottom so that zags start at the bottom. All modules start and end at the bottom in zags; note that nothing has to be transferred between modules. That is, instances of H, L, and R fold into `Hn`, `Lbn`, and `Rb`, respectively. Below the brick `Hxc`, an instance of F folds into `Fy`, where $y = (x + c) \bmod 2$.

3.6 Rule set

The rule set of the proposed counter consists of the following 377 rules:

(1,6),	(13,72),	(29,32),	(65,68),	(88,93),
(1,74),	(13,81),	(29,33),	(65,69),	(89,93),
(1,75),	(14,18),	(29,40),	(65,84),	(91,130),
(1,77),	(14,29),	(29,60),	(67,131),	(91,96),
(1,80),	(14,30),	(29,69),	(67,72),	(92,96),
(1,81),	(15,28),	(30,32),	(67,84),	(93,130),
(1,84),	(15,39),	(30,33),	(67,88),	(93,132),
(1,93),	(15,72),	(30,39),	(68,72),	(94,99),
(2,21),	(15,76),	(30,40),	(68,83),	(95,97),
(3,130),	(15,81),	(30,60),	(68,84),	(95,98),
(3,131),	(15,90),	(31,36),	(68,87),	(96,130),
(3,64),	(15,91),	(31,65),	(69,130),	(96,132),
(3,65),	(16,21),	(32,35),	(69,131),	(97,102),
(3,84),	(16,27),	(32,36),	(70,75),	(97,108),
(3,91),	(16,38),	(32,37),	(70,81),	(97,126),
(3,93),	(16,39),	(32,38),	(70,87),	(98,102),
(3,95),	(16,71),	(32,56),	(71,74),	(98,106),
(4,21),	(16,72),	(32,57),	(71,75),	(98,107),
(4,83),	(17,20),	(33,35),	(71,81),	(98,108),
(4,84),	(17,21),	(33,47),	(71,86),	(99,106),
(4,9),	(17,26),	(33,48),	(71,87),	(99,127),
(5,20),	(17,27),	(33,61),	(72,79),	(99,129),
(5,8),	(17,70),	(33,63),	(72,80),	(100,105),
(5,85),	(17,88),	(33,64),	(73,78),	(101,104),
(5,9),	(18,25),	(34,39),	(73,80),	(101,124),
(5,90),	(18,27),	(34,45),	(73,81),	(101,125),
(5,91),	(18,67),	(34,46),	(73,84),	(102,123),
(6,15),	(18,69),	(34,47),	(73,88),	(103,108),
(6,19),	(18,70),	(34,58),	(74,77),	(103,113),
(6,81),	(18,71),	(34,63),	(74,78),	(103,114),
(6,82),	(18,72),	(34,64),	(74,83),	(103,122),
(6,83),	(18,88),	(35,39),	(74,84),	(103,123),
(6,84),	(19,24),	(36,43),	(74,87),	(104,107),
(6,91),	(19,26),	(36,44),	(75,132),	(104,108),
(6,92),	(19,71),	(36,45),	(75,83),	(104,113),
(7,12),	(19,81),	(36,60),	(75,96),	(104,115),
(7,13),	(20,23),	(36,64),	(76,81),	(106,111),
(7,18),	(20,24),	(37,42),	(76,87),	(107,109),
(7,83),	(21,37),	(37,43),	(76,93),	(107,110),
(7,89),	(22,27),	(38,41),	(76,95),	(108,124),
(8,11),	(22,28),	(38,42),	(77,80),	(108,125),
(8,12),	(22,36),	(38,43),	(77,81),	(109,114),
(8,18),	(22,75),	(40,45),	(77,86),	(109,120),
(8,73),	(22,76),	(40,58),	(77,87),	(109,123),
(8,78),	(22,78),	(41,43),	(77,92),	(110,113),
(8,87),	(23,26),	(41,44),	(77,93),	(110,114),
(9,17),	(23,27),	(41,45),	(78,127),	(110,119),
(9,72),	(23,28),	(41,57),	(78,132),	(110,120),
(9,73),	(23,73),	(42,54),	(78,99),	(111,117),
(9,83),	(23,74),	(42,56),	(79,84),	(112,117),

(9,86),	(23,75),	(43,48),	(79,88),	(113,116),
(9,87),	(24,71),	(44,47),	(79,90),	(113,117),
(10,15),	(24,72),	(44,48),	(79,96),	(114,122),
(10,67),	(25,30),	(45,51),	(79,97),	(115,120),
(10,79),	(25,60),	(46,51),	(79,98),	(116,120),
(10,81),	(25,69),	(47,49),	(80,83),	(118,121),
(10,85),	(25,73),	(47,50),	(80,84),	(118,123),
(11,14),	(26,29),	(47,51),	(80,88),	(119,121),
(11,15),	(26,30),	(48,50),	(80,89),	(119,122),
(11,64),	(26,31),	(49,53),	(80,95),	(119,123),
(11,66),	(26,65),	(49,54),	(80,96),	(120,123),
(11,78),	(26,66),	(52,57),	(81,132),	(121,126),
(12,33),	(26,69),	(55,60),	(81,89),	(122,126),
(12,61),	(26,70),	(58,63),	(81,96),	(124,129),
(12,63),	(26,71),	(59,62),	(82,87),	(125,127),
(12,64),	(26,72),	(59,63),	(82,93),	(125,128),
(12,65),	(27,35),	(60,66),	(82,94),	(125,129),
(12,66),	(27,36),	(60,69),	(82,95),	(126,129),
(12,77),	(27,64),	(61,66),	(83,86),	(126,130),
(12,78),	(27,66),	(61,67),	(83,87),	(127,129),
(12,81),	(27,67),	(61,68),	(83,92),	(127,132),
(12,88),	(27,68),	(61,69),	(83,93),	(128,130),
(13,18),	(27,69),	(62,65),	(84,131),	(128,131),
(13,30),	(28,33),	(62,66),	(84,93),	(128,132).
(13,31),	(28,35),	(64,69),	(85,130),	
(13,32),	(28,60),	(64,85),	(85,90),	
(13,33),	(29,31),	(65,67),	(86,90),	

4 Conclusion

In this paper, we have expanded the existing finite binary counter by equipping it with a function of bit expansion at an overflow. This capability of handling overflows enables the system to launch at a simplest possible seed that encodes nothing but a Turn Signal for the first right carriage-return as long as the system starts counting from 0 (see Fig. 13).

The infinite counter was used to simulate countably many Turing machines in parallel for proving the undecidability of problems on aTAM in Bryans et al. (2013); Lathrop et al. (2011). The inherent sequentiality of oritatami prevents the proposed counter from being utilized alike or at least makes such applications highly non-trivial. The real significance of this counter in practice is that it can be embedded into a large-scale system as a counting module that can transition at an overflow into another phase, which does not have to do bit-expansion. A two-phase oritatami system to self-assemble the $n \times n$ square is under construction; starting from an $O(\log n)$-size seed on which an initial counter value is encoded, it first counts up to $2^{\log n}$ while drawing the diagonal, and at an overflow, it changes the direction of counting at 90 degrees and keeps just drawing diagonally until the diagonal reaches the right end of the counter. It is preferable to optimize this counter in these applications, for example, by reducing bead types, shortening the period, or simplifying its rule set, though such optimization problems are computationally hard in general (Han and Kim 2019; Ota and Seki 2017).

Acknowledgements This work is supported in part by KAKENHI Grant-in-Aid for Challenging Research (Exploratory) No. 18K19779, for Scientific Research (B) No. 20H04141, and Scientific Research (C) No. 20K11672, and JST Program to Disseminate Tenure Tracking System No. 6F36, both granted to S. S.

References

Adleman L, Chang Q, Goel A, Huang M.D (2001) Running time and program size for self-assembled squares. In: Proceedings of STOC 2001, ACM. pp 740–748

Bryans N, Chiniforooshan E, Doty D, Kari L, Seki S (2013) The power of nondeterminism in self-assembly. Theory Comput 9:1–29

Demaine ED, Hendricks J, Olsen M, Patitz MJ, Rogers TA, Schabanel N, Seki S, Thomas H (2018) Know when to fold 'em: Self-assembly of shapes by folding in oritatami. In: Proceedings of DNA24. LNCS, vol. 11145, pp 19–36. Springer

Elonen A (2016) Molecular folding and computation. Bachelor Thesis

Evans CG (2014) Crystals that Count! Physical Principles and Experimental Investigations of DNA Tile Self-Assembly. Ph.D. thesis, Caltech

Geary C, Andersen ES (2014) Design principles for single-stranded RNA origami structures. In: Proceedings of DNA 20. LNCS, vol. 8727, pp 1–19. Springer

Geary C, Étienne Meunier P, Schabanel N, Seki S (2018) Proving the Turing universality of oritatami cotranscriptional folding. In: Proceedings of ISAAC 2018. LIPIcs, vol. 123, pp. 23:1–23:13

Geary C, Étienne Meunier P, Schabanel N, Seki S (2019) Oritatami: A computational model for molecular co-transcriptional folding. Int. J. Mol. Sci. 20(9):2259 (**preliminary version published in MFCS 2016**)

Geary C, Rothemund PWK, Andersen ES (2014) A single-stranded architecture for cotranscriptional folding of RNA nanostructures. Science 345(6198):799–804

Han YS, Kim H (2018) Construction of geometric structure by oritatami system. In: Proceedings of DNA24. LNCS, vol. 11145, pp 173–188. Springer

Han YS, Kim H (2019) Ruleset optimization on isomorphic oritatami systems. Theor Comput Sci 785:128–139

Lathrop JI, Lutz JH, Patitz MJ, Summers SM (2011) Computability and complexity in self-assembly. Theory Comput Syst 48(3):617–647

Masuda Y, Seki S, Ubukata Y (2018) Towards the algorithmic molecular self-assembly of fractals by cotranscriptional folding. In: Proceedings of CIAA 2018. LNCS, vol. 10977, pp 261–273. Springer

McClung CR (2006) Plant circadian rhythms. The Plant Cell 18:792–803

Minsky M (ed.) (1967) Computation: Finite and Infinite Machines. Prentice-Hall, Inc

Ota M, Seki S (2017) Ruleset design problems for oritatami systems. Theor Comput Sci 671:26–35

Pchelina D, Schabanel N, Seki S, Ubukata Y (2020) Simple intrinsic simulation of cellular automata in oritatami molecular folding model. In: Proc. LATIN 2020. LNCS, vol. 12118, pp 425–436. Springer

Rothemund PWK, Winfree E (2000) The program-size complexity of self-assembled squares (extended abstract). In: Proceedings of STOC 2000, ACM. pp 459–468

Winfree E (1998) Algorithmic Self-Assembly of DNA. Ph.D. thesis, Caltech